Metric-Based Classification of Graph Vertices

Daniel Kim, John Pugmire

A report submitted in partial fulfillment of the requirements for the degree of Bachelor of Science

Advisors: Padraig Ó Catháin, Robert J Walls

Worcester Polytechnic Institute
United States of America
April 25, 2019

Acknowledgements

We would like to thank Professor Padraig Ó Catháin and Professor Robert J. Walls for their guidance and support throughout the duration of this project.

Abstract

In their 2013 paper, Cao et. al introduce the diffusion state distance (DSD) metric on graphs for use in the vertex labeling problem on protein-protein interaction networks. We generalize their classification approach, which uses weighted k-nearest neighbors voting, to work with any graph metric. We analyze the performance of this approach on graphs resembling real-world networks using shortest-path distance, DSD, and resistance distance. To this end, we propose novel simulation models to generate labeled scale-free and small-world networks, and perform label prediction experiments on the simulated graphs as well as real-world networks. We conclude that the DSD-based prediction algorithm exhibits more robust community awareness than the ones using the other metrics.

Contents

Chapter 1

Introduction

An abundance of network data has led to many studies on predicting information about vertices in networks. Such studies are important because they can lead to recommendation systems [10], classification of vertices in the network, the prediction of protein function, and many other useful applications. Many graph-based approaches have been considered for prediction on networks, as networks have a natural relation to graphs. In this project, we focus on a specific method of prediction, previously used in a biological network, and try to prove why it is more useful for prediction in certain networks than other methods of prediction.

Suppose we have a graph in which every vertex belongs to a unique class and a map from a proper subset of vertices to labels corresponding to their classes. Given such a graph, we define the vertex label prediction problem as predicting the missing labels in this graph. This problem has great practical importance. Data with a network structure is ubiquitous in real problems involving social media, the world wide web, and the biology of genes and proteins, and label prediction presents interesting possibilities [9].

One such possibility is presented by protein protein-interaction (PPI) networks. A PPI network is a graph where each vertex represents a protein and edges are drawn between any two proteins which are known to interact. In this case, some proteins are labeled based upon their function in the organism, and the task is to predict functions for the unlabeled proteins based upon the PPI network. To tackle this problem, Cao, Zhang, Park, Daniels, Crovella, Cowen, and Hescott developed a new metric on graph vertices, the diffusion state distance (DSD). They used the DSD to build a predictor that provided better performance of protein function predictors than competing methods based upon shortest path distance [5].

The goal of our project was to further explore graph-metric-based classification approaches in order to better understand the aspects of graph structure to which DSD reacts in comparison to other graph metrics. To accomplish this, we generalize the weighted nearest neighbors prediction method used by Cao et al. to use arbitrary graph metrics, and then performed a number of classification experiments using both simulated and real-world data sets.

We succeeded in developing novel generative models for labeled graphs which have a recoverable community structure. In addition, we show that DSD-based classification is more robust to noise and performs better all around than the other metrics do in a variety of different classification experiments. We conclude that the DSD is a robust and meaningful measurement of distance on graphs with certain sorts of underlying community structure.

Chapter 2 provides the background in graph theory needed to understand our methods, while Chapter 3 presents the novel data simulation models developed to test vertex label prediction algorithms. In Chapter 4, we develop background in metrics on graphs, particularly the DSD. These metrics are the keystone of our weighted nearest neighbors label prediction approach, which is described in Chapter 5 alongside a discussion of related machine learning methods of graphs.

Chapter 6 details the methods, results, and analyses of a suite of classification experiments performed on data simulated using the models described in Chapter 3. Chapter 7 builds upon these results with further experiments run on two real data sets.

Chapter 2

Graph Theory

In this chapter, we lay out the necessary background in graph theory for our later results. Section 2.1 includes fundamental definitions from graph theory and some important results from spectral graph theory, while Section 2.2 introduces small world and scale-free networks, which are graphs that have particular structural properties often found in real-world data. Finally, Section 2.3 provides definitions relating to random graphs and relevant examples of generative models.

2.1 Elementary Graph Theory

We begin by recalling some conventional definitions and notations from graph theory.

Definition 2.1. A **graph** G is a pair of sets (V, E) such that $E \subseteq \{\{x, y\} | x, y \in V\}$. We call V the set of **vertices** of G and E the set of **edges** of G.

Example 2.2 (The Pentagon)**.** The **pentagon**, also known as the **5-cycle**, is the graph (V, E) defined by $V = \{0, 1, 2, 3, 4\}$ and $E = \{\{0, 1\}, \{1, 2\}, \{2, 3\}, \{3, 4\}, \{4, 0\}\}$.

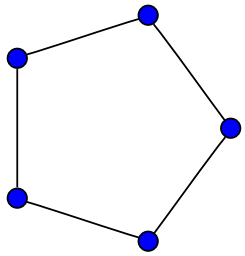

Figure 2.1: The Pentagon

Remark (Notation)**.** Let $G = (V, E)$ be a graph.

- For convenience, we will use subscript notation to refer to the edge and vertex sets of G, i.e. $V_G = V$ and $E_G = E$.
- $v \in G$ is an equivalent statement to $v \in V_G$
- $|G|$, called the **order** of G, is equal to $|V_G|$.

When we speak about graphs, we are concerned with the structure of the graph rather than the specific symbols in its vertex set. Thus we use the following definition of equivalence.

Definition 2.3 (Equivalence of graphs)**.** Two graphs G and H are equivalent if there exists a bijection $\phi : V_G \to V_H$ such that $\{u, v\} \in G$ if and only if $\{\phi(u), \phi(v)\} \in H$.

Equivalence of graphs induces an equivalence relation on the set of all graphs. For convenience, we will often only discuss graphs up to this equivalence relation (which only affects vertex labels).

Example 2.4. The **empty graph** of order n is the graph such that $|V| = n$ and $E = \varnothing$.

The **complete graph** of order n, denoted K_n, is the graph containing every possible edge, so that $|E_{K_n}| = \frac{n(n-1)}{2}$.

We say a graph is **bipartite** when there exists a bipartition of its vertex set such that there are no edges between vertices in the same part. The **complete bipartite graph**, denoted $K_{n,m}$, is such a graph where the two partitions have cardinality n and m respectively, and every pair of vertices in distinct partitions is joined by an edge.

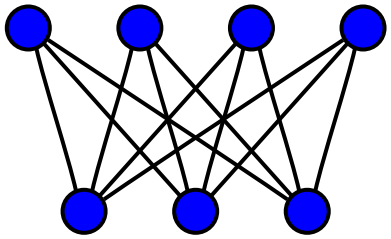

Figure 2.2: The complete bipartite graph $K_{3,4}$

Definition 2.5. The **neighborhood** of a vertex $u \in G$, denoted $N(u)$, is the set of all vertices v such that $\{u, v\} \in E_G$, and these v are called the **neighbors** of u. The **degree** of u is defined by $\deg(u) = |N(u)|$. A graph in which every vertex has the same degree is **regular**. If that degree is equal to k, then the graph is said to be k-**regular**.

Example 2.6. K_n is an $(n-1)$-regular graph, $K_{n,n}$ is an n-regular graph, and the pentagon is a 2-regular graph.

Definition 2.7. A **walk** of a graph G is an alternating sequence of edges and vertices such that each vertex is incident to the edges before and after it.

A **path** is the sequence of edges in a walk where every vertex is unique.

The **shortest-path distance** between two vertices $u, v \in G$, denoted $\mathrm{d}(u, v)$, is the minimum number of edges in a path from u to v.

Definition 2.8. The **adjacency matrix** A of a graph G is given by

$$A_{ij} = \begin{cases} 1 & : \{v_i, v_j\} \text{ is an edge in } G \\ 0 & : \text{otherwise} \end{cases}$$

where the set $\{v_i\}_{i=1}^{|G|}$ is an ordering of the vertices in G.

Note that the adjacency matrix of a graph is not unique in general. Depending on the way that the vertices of G are numbered, we may end up with a different matrix. However, for every adjacency matrix the following holds:

Definition 2.9. A matrix is **reducible** if and only if it can be put in block upper triangular form by simultaneous row and column permutations. In other words, a matrix M is reducible if and only if there exists a permutation matrix P such that $P^{-1}MP$ is block upper triangular. Otherwise, it is said to be **irreducible**.

Proposition 2.10. Let A be the adjacency matrix of a graph G. Then the following are true:

(1) A is symmetric (so the eigenvalues of A are real)

(2) A corresponds to a graph that is unique up to equivalence

(3) A is irreducible if and only if G is connected

Proof. We omit proofs for (1) and (2) as they are self-evident.

For (3), we first observe that $P^{-1}AP$ is an adjacency matrix of a graph equivalent to G for any permutation matrix P. So without loss of generality, suppose that G is connected and A is already in block upper triangular form. Then because A is symmetric, we have

$$A = \begin{bmatrix} B & \mathbf{0} \\ \mathbf{0} & C \end{bmatrix}$$

where B, C, are square block matrices. Say that B has size $m \times m$. It is clear that there are no edges connecting the vertices in $\{1, ..., m\}$ to those in $\{m+1, ..., n\}$. Thus G is not connected, which is a contradiction. □

The irreducibility result allows us to apply the Perron-Frobenius Theorem, resulting immediately in these additional properties of A.

Theorem 2.11 (Pg 673 (section 8.3) of [14])**.** *Let A be an irreducible nonnegative square matrix of order n. The following is true.*

(1) Let r be the maximum magnitude of the eigenvalues of A. Then r is a (real, positive) simple eigenvalue of A.

(2) The eigenvalue r has left and right eigenvectors whose components are all positive

(3) The only eigenvectors of A whose components are all positive have eigenvalue r.

(4)

$$\min_i \sum_j a_{ij} \leq r \leq \max_i \sum_j a_{ij}$$

Because A is nonnegative and irreducible for all connected graphs, these properties hold for all such adjacency matrices. Indeed, the irreducibility and nonnegativity of A yield many other interesting properties which we omit here.

Definition 2.12. The **spectral gap** of a matrix A is $\max_{i,j} |\lambda_i - \lambda_j|$, where λ_i and λ_j are the two largest eigenvalues of G.

The **spectral gap of a graph** is the spectral gap of its adjacency matrix.

We will next explore graph Laplacians, whose spectra are closely related to those of adjacency matrices.

Definition 2.13. The **degree matrix** of G is the diagonal matrix defined by

$$D_{ij} = \begin{cases} \deg(i) & : i = j \\ 0 & : i \neq j \end{cases}$$

Definition 2.14. The **graph laplacian** of G is given by $L = D - A$, where D is the degree matrix of G and A is the adjacency matrix. In other words,

$$L_{ij} = \begin{cases} \deg(i) & : i = j \\ -1 & : (i, j) \text{ is an edge in } G \\ 0 & : \text{otherwise} \end{cases}$$

Proposition 2.15. Let G be a k-regular graph, $\{\lambda_i\}$ and $\{x_i\}$ be the sets of eigenvalues and eigenvectors for its adjacency matrix A, and L be the graph Laplacian of G. Then

(1) $\{\lambda_i - k\}$ is the eigenvalue set of L, and

(2) $\{x_i\}$ is the eigenvector set of L

(3) L and A have the same spectral gap

Proof. Because G is regular, the degree matrix D is equal to kI. Let ant x_i be given. Then

$$\begin{aligned} Lx_i &= (A - D)x_i \\ &= \lambda_i x_i - kx_i \\ &= (\lambda_i - k)x_i \end{aligned}$$

Which simultaneously shows (1) and (2). (3) follows trivially from (1). □

2.2 Small-World and Scale-free Networks

Small-world networks are a class of graphs characterized by having a very small average shortest-path distance between any two vertices compared to the overall size of the graph.

Definition 2.16. The **characteristic path length** of a graph $G = (V, E)$ is the average distance between vertices in the graph, which is given by

$$L_G = \frac{1}{|E|} \sum_{\substack{u,v \in V \\ u \neq v}} \mathrm{d}(u, v)$$

where $\mathrm{d}(u, v)$ is shortest-path distance.

Definition 2.17 (Page 1 of [8])**.** Consider a graph $G = (V, E)$. G is a **small-world network** if $L_G \sim \log |V|$.

Small-world networks are ubiquitous in a variety of applications areas. However, many real-world examples of such graphs also have other distinctive structural properties which are not necessarily captured by their small-worldedness alone [2]. Thus, we introduce the following definition:

Definition 2.18 (Pg. 1 of [7])**.** A **scale-free network** is a graph whose vertex degrees follow a power law. That is, given a randomly selected $u \in G$, $P(\deg(u) = k) \sim k^{-\gamma}$ for some $\gamma > 0$.

One of the defining characteristics of power law distributions is that they have very long tails. In a scale-free graph with many vertices, this implies the existence of **hubs**, which we informally define as vertices whose degrees are far larger than average in the graph.

Real world examples of scale-free networks are abundant and include the world wide web, cellular communication networks, and protein-protein interaction (PPI) networks. It is not surprising, then, that scale-free networks are necessarily small-world networks, however we defer to Cohen and Havlin for proof of this fact.

Theorem 2.19 (Final result of [8])**.** *Scale-free networks are small-world networks.*

2.3 Random Graphs

Definition 2.20. A **random graph** is a random variable for which all outcomes are undirected graphs.

A **random graph process**, denoted (G_t), is a family of random graphs indexed by a discrete time $t \in \mathbb{N}$.

We are interested in random graph processes which build small-world networks. The Watts-Strogatz graphs are an example of such a process. They are defined by starting with a regular ring lattice and randomly rewiring edges until the graph is obtained.

Definition 2.21. An n-k **regular ring lattice** is a graph (V, E) with n vertices such that u, v is an edge if and only if $|u - v| \leq \frac{k}{2}$.

Definition 2.22. Let v be a vertex in a graph. We can **rewire** v by deleting one edge of v and drawing a new one by sampling uniformly from all vertices that do not share an edge with v.

Definition 2.23. Given a probability p and regular ring lattice parameters n and k, we define the (n, k, p) **Watts-Strogatz Process** as follows.

Let $r(G, v)$ be a random process that rewires vertex v in a graph G. We define a family of graphs, (G_t), by

$$G_{t+1} = \begin{cases} r(G_t, t) & : X \leq p \\ G_t & : X > p \end{cases}$$

for $t = 1, \ldots, |G|$, where G_0 is the n-k regular ring lattice, and X is a uniform random variable in the range $[0, 1]$. That is, we iterate over the vertices of the ring lattice and rewire each one with probability p.

We call graphs sampled from $G_{|n|}$ **Watts-Strogatz graphs**.

Watts and Strogatz showed empirically that the Watts-Strogatz graphs are small-world networks for all but extremely small values of p [16]. However, in general, they are not scale free networks [2], and thus do not show the structural characteristics of many practical data sets.

Definition 2.24 (Pg. 511 of [2])**.** Let any graph G_0 be given as well as some parameter m, $m \leq |G_0|$. We build the random graph G_{t+1} by adding a new vertex to G_t and connecting it to m vertices of G_t with probabilities proportional to the degree of each vertex. That is, the probability of adding an edge to a vertex u is

$$p_u = \frac{\deg(v)}{\sum_{v \in G_t} \deg(v)}$$

on the first step, and this is done a total of m times without replacement.

We call (G_t) the (G_0, m)-**Barabási-Albert (BA) process** and graphs sampled from G_n (G_0, m, n)-**Barabási-Albert (BA) graphs**.

This type of model, where edges to a new vertex are drawn with non-uniform probability, is known as **preferential attachment**.

Theorem 2.25 (Pg. 511 of [2])**.** ***Barabási-Albert graphs*** *are scale-free*

The scale-free-ness of BA graphs makes them an attractive model, as they are likely to have degree distributions similar to those of many real data sets. In addition, BA graphs are guaranteed to be connected.

Chapter 3

Random Labeled Graphs

We wish to use random graphs to test vertex classifiers. An issue that arises is that the generative models presented so far do not suggest any natural labeling for the vertices of the resultant graphs. Thus, we propose some models for generating labeled small-world and scale-free networks with a natural community structure.

Definition 3.1. A **labeled graph** is a graph G and a function $c : V_G \to S$, where S is an arbitrary finite set. For $u \in V_G$, we call $c(u)$ the **class** of u.

In considering labeled graphs, it is useful to look at not only at each vertex's degree, but also the number of neighbors with the same label vs the number of neighbors with a different label. For convenience, we define these quantities as follows:

Definition 3.2. Let G be a labeled graph, $u \in V_G$. The **same-class degree** of u, $\deg_{same}(u)$, is the number of neighbors of u in the same class as u. Similarly, $\deg_{diff}(u) = \deg(u) - \deg_{same}(u)$ is the number of neighbors in a different class.

3.1 Noisy Complete Components (NCC) Graphs

Definition 3.3. Let m be a natural number. We construct the **complete components graph** of order $n = 2m$ as follows. Let $V = \{1, 2, ..., 2m\}$, and then define E by

$$E = \{(u, v) : u, v \in \{1, ..., m\} \text{ or } u, v \in \{m + 1, ..., 2m\}\}$$

i.e. the disjoint union of two complete graphs of order m. In addition, we label the graph by the function

$$c(u) = \begin{cases} 0 & : u \in \{1, ..., m\} \\ 1 & : u \in \{m+1, ..., 2m\} \end{cases}$$

Definition 3.4. Let parameters (m, p, q) be given, $m \in \mathbb{N}$ and $p, q \in [0, 1]$, and let G_0 be the complete components graph of order $2m$. We construct a **Noisy Complete Components (NCC)** graphs as follows.

Iterate over ever pair of vertices in the graph (i.e. the edge set of K_{2m}). For every pair $\{u, v\} \in E_{G_0}$, that is, for the edges that already exist in G_0, we delete the edge with probability q. Likewise, for each pair $\{u, v\} \notin E_{G_0}$, we add the edge $\{u, v\}$ with probability p.

The resultant graph is an NCC graph. This definition generalizes easily to graphs with multiple components and components with different sizes, but the defined case will be sufficient for our purposes.

We will now inspect the properties of such graphs in order to demonstrate that they are, in fact, small worlds graphs in the subset of the parameter space in which we're interested. Before doing so, we recall some basic distributions from statistics.

Definition 3.5. A **Bernoulli distribution** with probability p is a discrete probability distribution with probability mass function

$$f(x) = \begin{cases} p & : \ x = 1 \\ 1 - p & : \ x = 0 \\ 0 & : \ \text{otherwise} \end{cases}$$

A **binomial distribution** of n trials with probability p, denoted $B(n, p)$ is equal to the sum of n independent bernoulli random variables with probability p. Its probability mass function is

$$f(x) = \binom{n}{x} p^x (1-p)^{n-x}$$

for $x = 0, 1, ..., n$ and 0 outside that range.

For a more complete discussion of these distributions and the probability theory employed in this chapter, see [6].

Theorem 3.6. *Let G be an (m, p, q) NCC graph and u a vertex in G. Then* $\deg(u)$ *follows the distribution $X + Y$, where X and Y are (independent) binomial random variables, $X \sim B(m-1, 1-q)$ and $Y \sim B(m, p)$. Moreover,* $\deg_{same}(u) = X$ *and* $\deg_{diff}(u) = Y$.

Proof. First, observe that adding and deleting edges while building an NCC graph is done independently for each edge. In other words, the existence or nonexistence of any edge of G is independent of every other edge. In addition, the number of edges added between u and all other different-class vertices is equal to a sum of m Bernoulli random variables of probability p, because there are m possible edges from u to the opposite class. Thus $\deg_{diff}(u)$ follows a binomial distribution on m trials, $\deg_{diff}(u) = Y \sim B(m, p)$.

In the case of same-class edges, we will consider the probability that an edge is *preserved* rather than deleted. Edges are preserved with probability $(1 - q)$, so as in the different-class case, we can see that the same-class degree of u follows a binomial distribution on $(m-1)$ trials, $\deg_{same} = X \sim B(m - 1, 1 - q)$.

As we've counted both the same- and different-class degrees, it is clear that $\deg(u) = X + Y$. □

We must take care to note that this is not the same thing as the degree distribution over the whole graph G. While each edge with respect to a single vertex is picked independently, this is not true over the whole graph, since each edge is connected to two vertices.

Remark. The previous theorem shows that the following is true

(1) $\mathbb{E}(\deg_{same}(u)) = (m-1)(1-q)$ and $\mathbb{E}(\deg_{diff}(u)) = mp$, where $\mathbb{E}$ is expectation.

(2) $\mathrm{Var}(\deg_{same}(u)) = (m-1)(1-q)q$ and $\mathrm{Var}(\deg_{diff}(u)) = mp(1-p)$, where Var is variance.

(3) $\mathbb{E}(\deg(u)) = (m-1)(1-q) + mp$ by linearity of expectation.

(4) $\mathrm{Var}(\deg(u)) = (m-1)(1-q)q + mp(1-p)$ by linearity of variance on independent random variables.

These graphs are extremely regular, so they do not exhibit scale-free properties. Thus, we also propose a variant on the Barabási-Albert model which adds labels while preserving the power law degree distribution.

3.2 Class-Weighted Barabási-Albert (CWBA) Graphs

Definition 3.7. Let parameters G_0 and $m \leq |G_0|$ be given as in the BA process as well as a finite set of labels S and a factor $\rho \geq 1$. In addition,

suppose each vertex in G_0 has been labeled by an element of S. Given a graph G_t, we build G_{t+1} as follows.

As in the BA process (see Definition 2.24, page 12), we will add one new vertex and draw edges using preferential attachment, however, we label our new vertex l, which is chosen from S with uniform probability. Then, we reweight the probability of drawing each edge in order to favor vertices with label l by a factor of ρ.

Define S_l to be the set of vertices with label l. Then, we define the probability of drawing an edge to a vertex u as

$$p_u = \begin{cases} \frac{\rho \deg(u)}{w} & : u \in S_l \\ \frac{\deg(u)}{w} & : u \in (V_G - S_l) \end{cases}$$

where w is the weighted degree sum,

$$w = \rho \sum_{v \in S_l} \deg(v) + \sum_{v \in (V_G - S_l)} \deg(v)$$

We call this random process the **class-weighted Barabási-Albert (CWBA) process** and we call graphs sampled from this model **CWBA graphs**.

We do not prove that CWBA graphs are scale-free, but degree plots over arbitrary choices of parameters suggest that they are. See Figure 3.1.

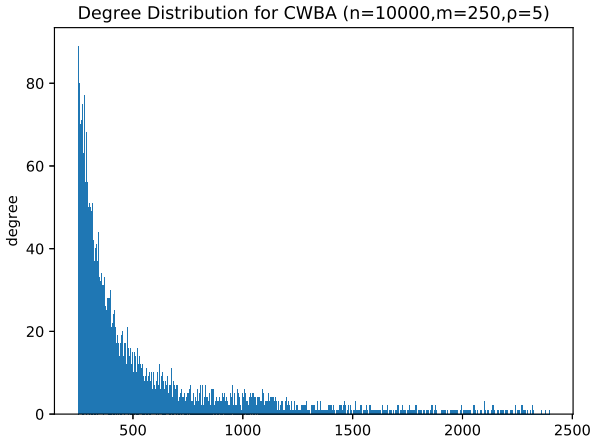

Figure 3.1: Degree distribution of CWBA graphs demonstrate scale-free behavior.

Between the apparent power law degree distribution and the straightforward reweighting of the preferential attachment algorithm, we expect label prediction experiments on CWBA graphs to be a reasonably good indicator of how an algorithm would perform on real-world data.

Chapter 4

Metrics on Graphs

In this chapter, we provide background about metrics on graph vertices, with a particular focus on the diffusion state distance (DSD). The three prediction algorithms compared in Chapters 6 and 7 are identical except for the choice of metric, as a key part of our project is understanding how that choice affects label prediction performance. For details about how our classification algorithm uses metrics to pick labels, see Chapter 5.

4.1 Definition and Shortest-Path Distance

A metric is a nonnegative real-valued function that generalizes Euclidean distance between points in $\mathbb{R}^n$ to general sets. In our case, the set is the vertices of the graph, and in the context of the label prediction problem, we use metrics to determine similiarity of two vertices in the graph.

Definition 4.1. A **metric** on a set S is a function $f : S \times S \to \mathbb{R}$ satisfying

(1) $f(u, v) \geq 0 \ \forall u, v \in G$,

(2) $f(u, v) = 0 \iff u = v$ (identity of indiscernables),

(3) $f(u, v) = f(v, u) \ \forall u, v \in G$, and

(4) $f(u, v) \leq f(u, w) + f(v, w) \ \forall u, v, w \in G$ (triangle inequality).

The standard metric on graphs is the shortest-path distance (Definition 2.7), whose definition we reiterate here for convenience. The **shortest-path distance** between two vertices $u, v \in G$, denoted $\mathrm{d}(u, v)$, is the minimum number of edges in a path from u to v.

Proposition 4.2. Shortest-path distance is a metric (on the vertices of connected graphs).

Proof. From the definition of shortest-path distance, it is clear that metric conditions (1), (2), and (3) are satisfied, since we're dealing with unweighted, undirected graphs.

To prove (4), let any three vertices in a connected graph u, v, w be given. Define $a = \mathrm{d}(u, w)$ and $b = \mathrm{d}(v, w)$. Then there exists a path from u to w of length a and from w to v of length b, and concatenating these paths gives a path from u to v of length $a + b$. Thus, by definition of shortest-path distance, $\mathrm{d}(u, v) \leq a + b = \mathrm{d}(u, w) + \mathrm{d}(v, w)$ for any three vertices u, v, w, which is more than sufficient to show (4). □

4.2 Resistance Distance

Definition 4.3 (from [17])**.** Let G be a connected graph. Imagine that G is an electrical network where every edge is a 1-ohm resistor. The resistance distance between $u, v \in G$, denoted $\Omega(u, v)$, is the reciprocal of the resistance between u and v as calculated by Kirchoff's laws, with the unit (ohms) dropped.

Formally, we can define it as follows. Let L be the graph laplacian of G and define Γ as

$$\Gamma = L + \frac{\mathbf{1}}{n}$$

where $\mathbf{1}$ is the matrix consisting of all 1s. Then,

$$\Omega(u, v) = (\Gamma)^{-1}_{ii} + (\Gamma)^{-1}_{jj} - 2(\Gamma)^{-1}_{ij}$$

Theorem 4.4 (Page 89, Theorem B of [12])**.** *Ω is a metric (on the vertices of an arbitrary connected graph)*

Resistance distance is another example of a metric on graphs, and it is dramatically different from shortest-path distance. One of its key characteristics is that as we add more paths connecting two vertices, the distance between them decreases [12]. Because resistance distance gives consideration to the entire graph (as opposed to just the shortest path), we expect it to be more stable to noise in the form of randomly added or deleted edges than shortest path.

4.3 Diffusion State Distance

The diffusion state distance (DSD) is a metric on graphs which determines distance between two vertices based upon the convergence behavior of random walks starting from each vertex. Intuitively, it provides a way to measure vertex distance that is sensitive to the local structure of the graph, and appears to be well suited to detecting community structures in graphs.

In the original paper, Cao, Zhang, Park, Daniels, Crovella, Cowen, and Hescott define DSD in terms of a vector-valued function $\mathrm{He}^k(u)$, which computes the expected number of times a length-k random walk originating at a vertex u will visit each other vertex in the graph. They compute DSD by taking the l_1-norm of the difference between two such vectors in the limit as $k \to \infty$. We present an alternative definition which is easier to manipulate with the usual machinery of linear algebra. We begin by recalling some definitions.

Definition 4.5. A **random walk** of a graph is a walk (see Definition 2.7) originating at some vertex in which each edge is picked uniformly randomly from all the edges adjoined to the vertex preceding it.

Definition 4.6 (Page 302 of [4])**.** A (discrete-time) **markov chain** on a finite set of states V is a sequence of random variables $X_0, X_1, ...$ taking values $x_o, x_1, ... \in V$ such that for a given t, the probability of each outcome of X_{t+1} depends only on x_t (the outcome before it).

Let $u, v \in V$. Then the conditional probability $P(X_{t+1} = v | X_t = u)$ is called the **transition probability** from u to v.

The **transition matrix** of a markov chain is the matrix T given by

$$T_{ij} = \text{The probability of transitioning from state } j \text{ to state } i$$

Random walks may be modeled as markov chains where the states are the vertices in the graph. The random walk transition matrix of a graph G can be written $T = AD^{-1}$, where A is the adjacency and D is the degree matrix, (Definitions 2.8 and 2.13). For our purposes, we assume that vertices are labeled by the positive integers $1, 2, ..., n$ and that the rows and columns of G correspond to this ordering.

Proposition 4.7 (Properties of T)**.** Let G be a graph and T the transition matrix for the corresponding random walk markov chain. The following is true:

(1) T is irreducible

(2) every eigenvalue of T has magnitude ≤ 1

Proof. To show (1), we first recall from Proposition 2.10 that the adjacency matrix is irreducible. From the definition $T = AD^{-1}$, we can see that T has zeros in the same set of indices as A, and so must be irreducible by analogous argument.

(2) follows from (1) and application of the Perron-Frobenius Theorem (Theorem 2.11). □

Based on how we've defined the transition matrix, it can be thought of as an operator which takes a marginal distribution of states in the markov chain, and outputs the marginal distribution after one step. So, the marginal distribution of vertices in the k^{th} step of a random walk originating from vertex u is given by $T^k e_u$, where e_u is the u^{th} standard basis vector in $\mathbb{R}^n$, $e_{u,u} := 1$ and $e_{u,j} := 0, u \neq j$ for $u = 1, ..., n$.

Finally, we can define DSD.

Definition 4.8. Let G be a graph, $u, v \in G$. The **diffusion state distance (DSD)**, denoted $\delta(u, v)$, is defined by

$$\delta(u, v) = || \sum_{k=0}^{\infty} T^k e_u - T^k e_v ||_1$$

where T is the transition matrix of G's random walk markov chain and e_i is th i^{th} standard basis vector in $\mathbb{R}^n$.

Theorem 4.9 (Page 7 of [5])**.** *DSD is a metric.*

We defer to Cao et. al for proof of this.

As compared to shortest-path distance, we would expect DSD to be more resilient to random noise in the form of randomly added and deleted edges. This is because DSD considers the structure of the entire graph instead of just the shortest path. Resistance distance is also computed using the whole graph, so we would expect that to be similarly resilient. However, DSD appears to be measuring the similarity of two vertices' neighborhoods by comparing random walk convergence behavior, whereas resistance distance is measuring electrical current capacity between two vertices. In the context of most label prediction problems, where labels correspond to communities, this suggests intuitively that DSD superior.

4.4 DSD on the Complete Graph

In this section, we work through the problem of computing DSD on the complete graph. This is not a particularly illuminating result, but we hope it will help to familiarize the reader with the DSD.

Consider the complete graph K_n. In this case, $D = (n-1)I$ and $A = (J - I)$, so our transition matrix T is given by $\frac{1}{n-1}(J - I)$. In order to compute $T^k e_u$ in the limit, we will represent e_u as a linear combination of eigenvectors of A.

Proposition 4.10. The all-ones vector 1_n is an eigenvector of T with eigenvalue $\lambda = 1$, and every vector $x \in \mathbb{R}^n$ such that $\sum_i x_i = 0$ is an eigenvector of T with $\lambda = -\frac{1}{n-1}$.

Proof. Multiplying a vector by the all-ones matrix takes the sum of that vector's values for every index in the result, so $J \cdot 1_n = n \cdot 1_n$. Similarly $Jx = 0_n$, for any x s.t. $\sum_i x_i = 0$. Thus,

$$\begin{aligned} T \cdot 1_n &= \frac{1}{n-1}(J - I) \cdot 1_n \\ &= \frac{1}{n-1}(n \cdot 1_n - 1_n) \\ &= 1_n \end{aligned}$$

and

$$\begin{aligned} Tx &= \frac{1}{n-1}(J - I)x \\ &= \frac{1}{n-1}(0_n - x) \\ &= -\frac{1}{n-1}x \end{aligned}$$

□

Next, we will show how to write any e_u as a linear combination of eigenvectors of T. We define α_u by $\alpha_{u,u} := n - 1$ and $\alpha_{u,j} = -1, u \neq j$. The entries of α_u sum to 0, so $T\alpha_u = -\frac{1}{n-1}\alpha_u$. We can write $e_u = \frac{1}{n}(1_n + \alpha_u)$.

Corollary 4.11. The eigenvectors of $J - I$ span $\mathbb{R}^n$.

Proof. Since all standard basis elements e_j of $\mathbb{R}^n$ can be expressed as linear combinations of eigenvectors for $J-I$, the eigenvectors of $J-I$ span $\mathbb{R}^n$. $\square$

Theorem 4.12. *Let K_n be the complete graph with nodes labelled $1, ..., n$. Then for any two distinct nodes u and v, $\delta(u,v) = \frac{2(n-1)}{n}$.*

Proof. We will use α_u as defined above. DSD is given by

$$\begin{aligned}
\delta(u,v) &= \sum_{k=0}^{\infty} ||T^k e_u - T^k e_v||_1 \\
&= \frac{1}{n} \sum_{k=0}^{\infty} ||T^k(1_n + \alpha_u - 1_n - \alpha_v)||_1 \\
&= \frac{1}{n} \sum_{k=0}^{\infty} ||T^k(\alpha_u - \alpha_v)||_1 \\
&= \frac{1}{n} \sum_{k=0}^{\infty} ||(-\frac{1}{n-1})^k(\alpha_u - \alpha_v)||_1 \\
&= \frac{||\alpha_u - \alpha_v||_1}{n} \sum_{k=0}^{\infty} (-\frac{1}{n-1})^k
\end{aligned}$$

Since $|-\frac{1}{n-1}| < 1$, the geometric series converges, $\sum_{k=0}^{\infty}(-\frac{1}{n-1})^k = \frac{n-1}{n}$. When $u \neq v$, the difference $\alpha_u - \alpha_v$ will have exactly two non-zero entries (since they are identical at all indices but u and v). These non-zero entries will be n at index u and $-n$ at index v. Thus, $||\alpha(u) - \alpha(v)||_1 = 2n$, and so

$$\begin{aligned}
\delta(u,v) &= \frac{2n}{n}(\frac{n-1}{n}) \\
&= \frac{2(n-1)}{n}
\end{aligned}$$

$\square$

Chapter 5

Label Prediction Methods on Graphs

In this chapter, we define label prediction methods and show how they can be applied on graphs. We present different problems we can solve using label prediction methods and how we can incorporate graph metrics, such as the diffusion state distance (DSD), into these methods. We use the terms label prediction methods and vertex classifiers interchangeably.

5.1 Problem Definition

We begin by presenting definitions relating to labels of graphs.

Definition 5.1. A **partially labeled graph** is a graph G and a function $c : V_{G_p} \to S$, where S is an arbitrary set of labels, and $V_{G_p} \subseteq V_G$ with $|V_{G_p}| = \lfloor p \cdot |V_G| \rfloor$, $0 \leq p \leq 1$.

The set $V_G \setminus V_{G_p}$ is called the set of **unlabeled** vertices of G.

The function c is called a **partial labeling** of G.

Definition 5.2. A **censoring** of a labeled graph G and its labeling function $c : V_G \to S$ is a set V_{G_c} and a function $c_p : V_G \setminus V_{G_c} \to S$ such that c_p is a partial labeling of G.

The function c of the labeled graph G is called the **ground truth labeling** of the censoring of G. Note that the set V_{G_c} is the set of unlabeled vertices of the partial labeling of G.

Given a partially labeled graph G, a censoring (V_{G_c}, c_{censor}) of G, and a ground truth labeling c_{gt} of G, a **label prediction method** is an algorithm

that attempts to correctly guess the labels of the unlabeled vertices V_{G_c} with respect to the ground truth labels $c_{gt}(v), v \in V_{G_c}$.

In order for a label prediction method on a graph to have any success, the ground truth labeling must reflect some underlying graph structure. If the labels in a graph were assigned at random to each vertex, a label prediction algorithm could not be expected to perform better than randomly guessing the labels on vertices.

5.1.1 Voting Algorithms

Cao, Zhang, Park, Daniels, Crovella, Cowen, and Hescott [5] describe a simple prediction method called the neighborhood majority voting algorithm. This algorithm considers each vertex with unknown label and has its neighbors vote on the label for the vertex. We considered two implementations of this algorithm, which differ in how they determine which neighbors vote. One implementation considers each vertex $v \in V$ and all neighbors of v within an ε distance from v (a ball of radius ε). The ε distance depends on the metric under consideration, and may be changed as a parameter. In an unweighted scheme, each neighbor within the ball of radius ε votes equally for their own label. In a weighted scheme, we must consider a metric on a graph to use (chapter 4). Using this metric, each neighbor gets a vote proportional to the reciprocal of its distance to the vertex v in consideration. The other implementation of this algorithm considers each vertex $v \in V$ and the k-nearest neighbors of v with respect to the graph metric. Voting is done similarly in both an unweighted and weighted scheme.

There are other prediction methods that exist, such as the χ^2 neighborhood algorithm, the multi-way cut algorithm, and the functional flow algorithm [5]. These prediction methods can also be modified to incorporate graph metrics discussed in chapter 4. However, we only consider the weighted majority voting algorithm for our simulations in order to keep the intuition behind results of this algorithm simple.

5.2 Real World Data

In this section, we discuss three different examples of graph-based studies performed on real world data. We discuss how these examples constructed graphs from their data, and what kind of studies were performed on the resulting graphs. These studies give constructions of different graph representations of data that we can use to test the effects of different metrics with prediction algorithms.

5.2.1 Protein-Protein Interaction (PPI) networks

Cao et al. [5] studied the prediction of protein functional labels on the *S. cerevisiae* protein-protein interaction (PPI) network. The authors constructed a graph using annotated physical interactions in this PPI network. Proteins corresponded to vertices, and an annotated physical interaction between two proteins corresponded to an edge. Cao et al. removed redundant edges and the largest connected component was selected, resulting in a graph of 4990 vertices and 74,310 edges. They also noted that PPI networks are known to resemble small-world networks, as they have a small maximum shortest path, and a small characteristic path length. This implies that most vertices in the graph are close to every other vertex in the graph. One reason for the closeness of vertices in PPI networks was due to hub vertices, which are vertices with very high degree, representing proteins that interact with many other proteins. Figure 5.1 shows an example of functional annotation using the DSD from Cao et al.

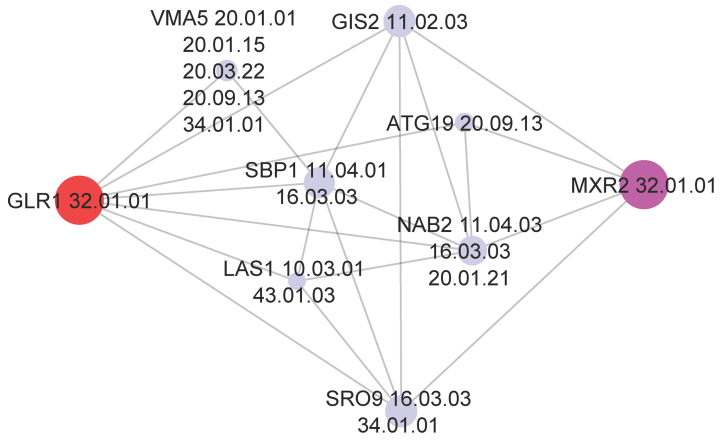

Figure 5.1: An example of functional annotation with the DSD metric from Cao et al. [5]. It is clear that the vertex colored purple is not a direct neighbor of the red vertex with respect to the shortest path distance metric. However, the purple vertex has a DSD distance closest to the red vertex, and they have the same label. Meanwhile, the direct neighbors of the purple vertex have different labels.

Cao et al. used four different prediction algorithms to compare the effectiveness of the DSD metric to that of the shortest path metric. Both weighted and unweighted majority voting algorithms, as well as the χ^2 neighborhood algorithm, multi-way cut algorithm, and functional flow algorithm were used

to compare the predictive performance of these metrics. The DSD metric was expected to perform better that the shortest path metric, since the small characteristic path length of the PPI network causes the notion of a shortest paths neighborhood to lose significance. All vertices in this network are close to every other vertex in the graph, so any neighborhood would contain a large portion of the vertices in the graph.

We used a similar approach in our project, studying the DSD metric and incorporating it into a label prediction algorithm.

5.2.2 Graph model for recommender systems

Huang, Chung, and Chen [10] introduce a generic graph model for e-commerce transaction data that can support various recommendation methods. The two-layer graph model proposed represents relationships between products and customers. In this model, each layer consists of vertices representing products or customers. Three types of edges in this two layer system capture the inputs to this model from real world data. Edges between two customers capture similarity based on available demographic data, answers to questionnaires, and web usage patterns. Edges between two products capture similarity using descriptions of the product. Finally, edges between customers and products capture transaction information such as purchase history, customer rating, and related browsing behavior. Figure 5.2 illustrates an example of the two-layer graph model.

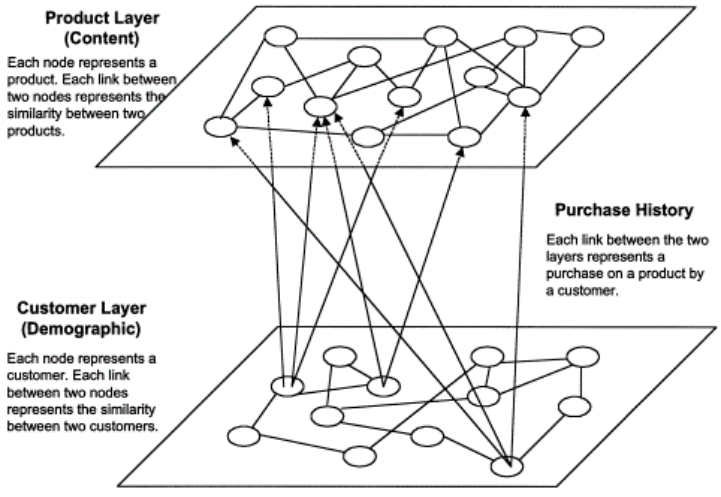

Figure 5.2: The two-layer graph model proposed by Huang, Chung, and Chen [10].

Huang, Chung, and Chen considered three different recommendation methods to use on the model mentioned previously. The direct retrieval method looks at a customer's previous purchases and products purchased by similar customers to retrieve products to recommend to the customer. The association mining method uses the purchase history of a customer to generate association rules about purchasing patterns in order to predict the customer's next purchases. The high-degree association retrieval method uses weights on edges to represent association strength and examines paths between the target customer vertex and a product vertex to calculate an association estimate and determine if the product should be recommended. Transactions from one of the largest online bookstores in Taiwan were used for data including 9695 books, 2000 customers, and 18,771 transaction records.

The two-layer graph model introduced by Huang, Chung, and Chen can be interpreted as a graph labeling problem. As a simple example, we can take the vertices and edges from just the customer layer of the two-layer model. Since the customer layer included information about demographic data and web usage patterns, we could label customers with age or certain websites visited and try to predict the labels of prospective customers. We can perform a similar analysis with the product layer as well as with the whole model including the interlayer edges.

Such a model can be very useful for advertisers who wish to come up with a strategic advertising plan. Assuming that an advertisement would have more success if it were shown to people more likely to buy the product being advertised, we can use the graph model to predict which customers would buy the product. The product layer can be used to find all products similar to the product being advertised. Then, we can construct a graph in which vertices are customers who had bought similar products, and edges existed between customers who had bought the same product. A prediction algorithm incorporating the DSD could be used to predict the customers who would buy the product if we knew a few customers that had already bought the product, or were very likely to buy the product. The DSD proved useful in filtering out hub vertices in the PPI networks, and it may be useful for e-commerce networks as well. Customers with a large amount of purchases may be less informative about product preferences than customers with fewer purchases.

Overall, this study shows that subject-knowledge can be used to create real world graphs (customer layer, product layer, purchase history). We can extend this to see how subject-knowledge can be used to determine weights during the voting process for label prediction methods. Labels can also be

determined from subject-knowledge. However, these labels must have an underlying structure or intuition behind them in order for label prediction algorithms to work.

5.2.3 Laplacian Eigenmaps

Belkin and Niyogi [3] propose an algorithm for constructing a locality-preserving representation of data sampled from a low dimensional manifold embedded in a higher dimensional space. An example can be found in $n \times n$ gray scale images of a fixed object taken by a moving camera. These images give data points in $\mathbb{R}^{n^2}$, but the inherent dimensionality of this data should be the number of degrees of freedom of the camera. The presented algorithm constructs a representation of the data that reduces the dimensionality of the data.

Belkin and Niyogi construct a weighted graph from a given set of points in $\mathbb{R}^n$. Each point is represented by a vertex, and edges are drawn between neighboring points. Neighborhoods can be determined using k nearest neighbors or ε-neighborhoods. Weights are determined using heat kernels, or simply adjacency. Finally, eigenmaps are used to reduce dimensionality of the data.

1000 binary 40×40 images of vertical and horizontal bars at arbitrary points were randomly chosen as data. The Laplacian Eigenmap algorithm and Principal Component Analysis (PCA) was applied to this data and compared. The Laplacian Eigenmap algorithm produced a data representation that clearly showed separate clusters for the vertical and horizontal bars, which PCA failed to do.

This study is quite different from the previous two studies. However, it still raises some interesting questions and challenges in relation to our project. The Laplacian Eigenmaps algorithm focused on being able to detect graph structure, assuming that the given data lies in a lower dimensional manifold. In our project, we try to detect properties of graph structure that allow prediction methods using the DSD to perform well. We could examine whether label prediction methods using the DSD would be able to detect information about these lower dimensional manifolds.

Chapter 6

Simulations

In this chapter, we discuss data collected from several simulations run on our Noisy Complete Components (NCC), Noisy Complete Components with Hubs (NCCH), and Class-Weighted Barabási-Albert (CWBA) models introduced in Chapter 3. We use these models because they are small-world and have an intuitive ground truth labeling of vertices. The simple structures of our models also allow us to test different parameters relating to graph structure and examine their effects on prediction accuracies.

For each model, we set a variety of parameters that we want to test. After constructing the graph, we censor a proportion ($censorP$) of the graph, then use a weighted k-nearest neighbors voting (Chapter 5) to solve a vertex label prediction problem. This process is repeated with the same parameters $avgRuns$ number of times, and the prediction accuracies obtained are averaged. We incorporate three different metrics on graphs (Chapter 4) to our weighted k-nearest neighbors voting algorithm: the diffusion state distance (DSD), shortest path distance (SPD), and resistance distance (RD).

6.1 Noisy Complete Components (NCC) Graphs

In this section, we construct NCC graphs (Chapter 3) and run label prediction methods on them.

6.1.1 Data Collection

Our NCC graphs have three input parameters, where m is the number of vertices in one complete component ($n = 2m$ total vertices), p is the probability of adding an edge between components, and q is the probability of

removing an edge within components.

$n\ (= 2m)$	500
p	Range from 0 to 1
q	0.5
$censorP$	0.7
$avgRuns$	10

(a) Fixed q

$n\ (= 2m)$	500
p	0.5
q	Range from 0 to 1
$censorP$	0.7
$avgRuns$	10

(b) Fixed p

Table 6.1: Tables of parameter values used in our NCC simulations. The table on the left shows simulation parameters for a fixed q, and the table on the right shows simulation parameters for a fixed p.

Table 6.1 shows the parameter values we used in our simulations. The value of parameter m was set to 250 because this was a sufficiently large value to allow us to observe differences in prediction accuracy. Figure 6.1 shows that the parameter m only increases the precision of the prediction accuracies. The parameters p and q were considered probabilities of adding noise to our models, so we ran simulations to test the effects of these parameters on prediction accuracies. Figure 6.1(c) shows a plot of the prediction accuracies over the range of values for p, with a fixed $q = 0.5$. Figure 6.2 shows a plot of the prediction accuracies over the range of values for q, with a fixed $p = 0.5$.

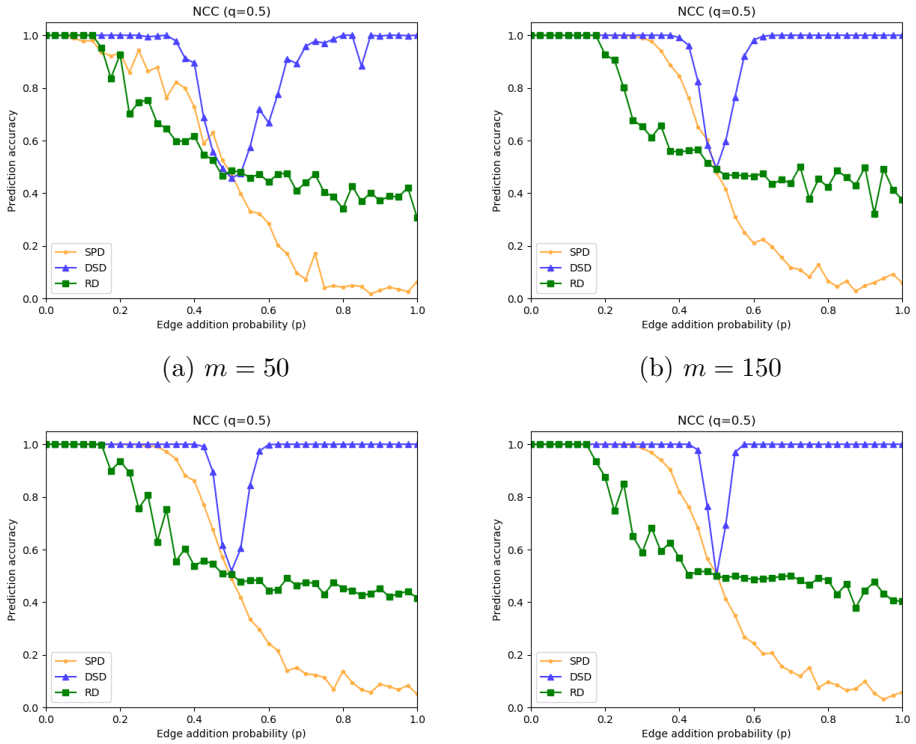

(a) $m = 50$ (b) $m = 150$

(c) $m = 250$ (d) $m = 550$

Figure 6.1: These plots show that varying the parameter m in NCC graphs does not change results and a value of $m = 250$ will be sufficiently large to observe differences in prediction accuracies. Figure (a) shows that a small value of m may give slightly noisy prediction accuracies due to the smaller number of examples that the prediction accuracies are calculated from.

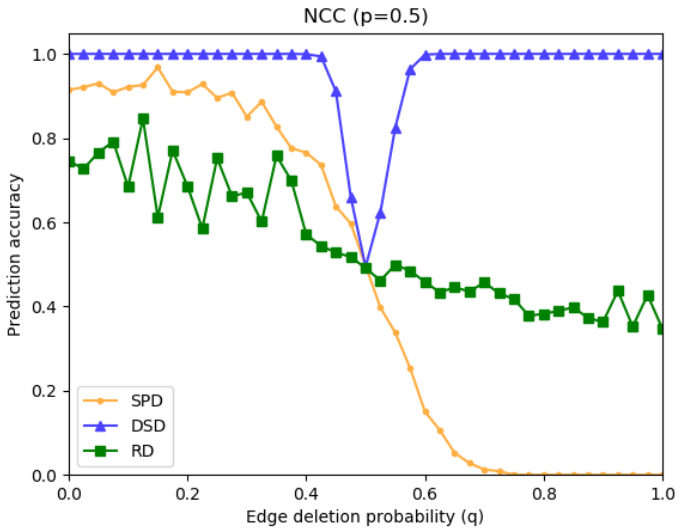

Figure 6.2: Plot showing prediction accuracies of the prediction method using the DSD, SPD, and RD metrics. In this simulation, the parameter p was fixed to 0.5, and m was set to 250. This plot suggests simulations are symmetric in p and q.

6.1.2 Analysis

It is important to note the structure of NCC graphs in extreme cases. For parameter $p = 0$ in NCC graphs (Chapter 3), there is zero probability of adding edges between components. Since we only consider the largest connected component in our analysis, we simply take one of the original components. If $p = 0$ and $q = 0$, then we get one complete component. This is not interesting, as all prediction methods should attain 100% prediction accuracy on these graph. For $p = 0$ and $q = 1$, we have a set of vertices and no edges. The largest connected component would be a single vertex. For $p = 1$, there exist edges from every vertex in one component to every vertex in the other component. For $p = 1$ and $q = 1$, we have a complete bipartite graph. We can expect that a prediction method using the shortest path distance with a small k value for the k-nearest neighbors prediction would result in very poor accuracy for this method. However, since we have just a binary labeling, these results can be flipped, making prediction using the inverse of the shortest path distance very effective. With $p = 1$ and $q = 0$, we have a complete graph where every vertex has equal same-class degree and

different-class degree. This case is not interesting as all prediction methods would give random results. This leads us to our next proposition.

Proposition 6.1. For $q = 1 - \frac{mp}{(m-1)}$, NCC graphs are Erdős-Rényi graphs with edge probability p.

Proof. We know that for NCC graphs (Chapter 3),

$$\mathbb{E}(\deg_{same}(u)) = (m-1)(1-q)$$

$$\mathbb{E}(\deg_{diff}(u)) = (m)p$$

If $q = 1 - \frac{mp}{(m-1)}$, then we get

$$\mathbb{E}(\deg_{same}(u)) = (m-1)(1-(1-\frac{mp}{(m-1)})) = mp$$

$$\mathbb{E}(\deg_{diff}(u)) = (m)p$$

Thus, we get

$$\mathbb{E}(\deg_{same}(u)) = \mathbb{E}(\deg_{diff}(u))$$

□

The NCC graph with parameters p, and $q = 1 - \frac{mp}{(m-1)}$ is expected to be close to an $(2mp)$-regular graph, where each vertex is expected to have the same number of same-class neighbors as different-class neighbors.

The expected number of same-class and different-class neighbors of a vertex u in an NCC graph corresponds to the expected same-class and different-class degrees from Chapter 3. So, from Theorem 3.6, we derive the following result.

Proposition 6.2. For two vertices u, v in an NCC graph,

(1) If u, v belong to the same class, they are expected to have

$$(m-2)(1-q)^2$$

common same-class neighbors, and

$$(m)p^2$$

common different-class neighbors.

(2) If u, v belong to different classes, they are expected to have

$$(2m-2)(1-q)p$$

common neighbors.

Proof. (1) We can see that if u, v belong to the same class, there are $(m-2)$ possible same-class vertices that could be common neighbors between them. Each of these vertices has a $(1-q)$ probability of being a same-class neighbor of u and a $(1-q)$ probability of being a same-class neighbor of v (chapter 3). Therefore, we get that the expected number of common same- class neighbors is $(m-2)(1-q)^2$.

Also, there are m possible different-class vertices that could be common neighbors between u and v. Each of these vertices has a p probability of being a different-class neighbor of u and a p probability of being a different-class neighbor of v. Therefore, we get that the expected number of common different-class neighbors is $(m)p^2$.

(2) If u, v belong to different classes, there are $(2m-2)$ possible vertices that could be common neighbors of u and v. Without loss of generality, each vertex has a $(1-q)$ probability of being a neighbor of u and a p probability of being a neighbor of v. Therefore, we get that the expected number of common neighbors is $(2m-2)(1-q)p$. □

Figure 6.1(c) shows that with a fixed probability of deleting edges within components of NCC graphs, and a range of probabilities of adding edges between components of NCC graphs, the label prediction method using the DSD outperforms the method using SPD and the method using RD. We can use expected values of same-class degrees (Chapter 3) to reason why such behavior occurs.

For a fixed $q = 0.5$, we can say for any vertex u,

$$\mathbb{E}(\deg_{same}(u)) = (249)(0.5)$$

$$\mathbb{E}(\deg_{diff}(u)) = (250)p$$

We can clearly see that for $p = 0.5$, the resulting graph will be random, having roughly the same number of same-class neighbors as different-class neighbors. This explains the near random prediction accuracies when p is close to 0.5. However, for $p < 0.5$, we can expect that $\mathbb{E}(\deg_{same}(u)) > \mathbb{E}(\deg_{diff}(u))$. In this case, the prediction method using SPD should predict with high accuracy, with a sharp decline as the value of p approaches 0.5. For

$p > 0.5$, the prediction method using SPD should predict with low accuracy, since $\mathbb{E}(\deg_{same}(u)) < \mathbb{E}(\deg_{diff}(u))$. Figure 6.1(c) shows this behavior of the prediction method using SPD.

The prediction method using DSD seems only to be affected by the p parameter when it approaches 0.5, and the graph becomes random. This behavior can be explained by the fact that the DSD cares about common neighborhoods when determining similarity, or distance. First we must note that all vertices in the NCC graph should be very similar to each other, since they all share the same $\mathbb{E}(\deg_{same}(u))$ and $\mathbb{E}(\deg_{diff}(u))$. This means that there is no point in differentiating between low-degree and high-degree neighborhoods for the NCC graphs. For $p < 0.5$, we know that $\mathbb{E}(\deg_{same}(u)) > \mathbb{E}(\deg_{diff}(u))$. This means that when looking at the neighborhoods of an arbitrary vertex u, a large number of common neighbors will be shared between vertices within the same component. Two vertices within the same component will share more common neighbors than two vertices in different components. This is also true for $p > 0.5$, where $\mathbb{E}(\deg_{same}(u)) < \mathbb{E}(\deg_{diff}(u))$. This means that the DSD between any two vertices within the same component is expected to be closer than two vertices in different components for most values of p given q is fixed.

The prediction method using RD performs the worst of the three metrics. Since the resistance distance considers the number of short paths between vertices when calculating distance, we can look at the short paths in NCC graphs. NCC graphs are very dense in edges, and because of the random probabilities of adding and deleting edges, it is difficult to obtain a structured notion of paths in this graph.

A similar analysis can be done for the simulation for a fixed $p = 0.5$ over the range of values for q, as shown in Figure 6.2.

6.2 Noisy Complete Components with Hubs (NCCH) Graphs

In this section, we construct NCCH graphs (Chapter 3) and run label prediction methods on them. We study these graphs in order to determine the effects of hub vertices on the prediction accuracies of NCC graphs. It is important to note that the hub vertices in NCCH graphs were labeled randomly.

$n\ (= 2m + hubs)$	500
p	Range from 0 to 1
q	0.5
$hubs$	100
$hubsP$	0.8
$censorP$	0.7
$avgRuns$	10

(a) Fixed q

$n\ (= 2m + hubs)$	500
p	0.5
q	Range from 0 to 1
$hubs$	100
$hubsP$	0.8
$censorP$	0.7
$avgRuns$	10

(b) Fixed p

Table 6.2: Tables of parameter values used in our NCCH simulations. The table on the left shows simulation parameters for a fixed q, and the table on the right shows simulation parameters for a fixed p.

6.2.1 Data Collection

We used the same values for similar parameters to the NCC graphs as described in the previous sections. The same process of fixing the parameter p or q in the NCC graphs was used.

The NCCH graphs have two more input parameters, *hubs* and *hubsP*, as shown in Table 6.2. The *hubs* parameter specifies the number of hub vertices to add, and the *hubsP* parameter specifies what proportion of the vertices in the complete components to add edges from each newly added hub vertex. A value of 0.8 was decided for the *hubsP* parameter in order to capture the idea of hub vertices and their large degrees. Figures 6.3 and 6.4 show our simulation results.

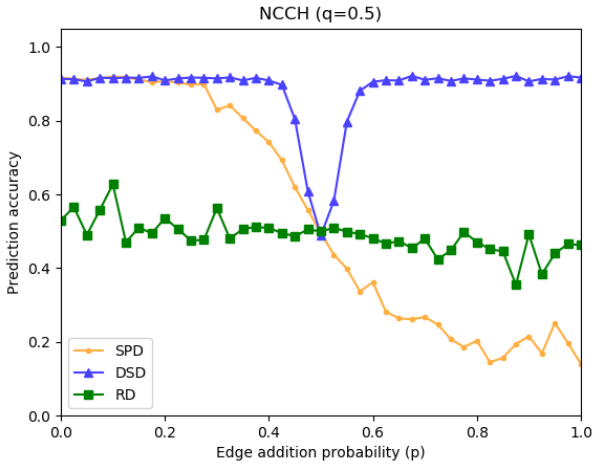

Figure 6.3: Plot showing prediction accuracies of the prediction method using the DSD, SPD, and RD metrics. In this simulation, the parameter q was fixed to 0.5.

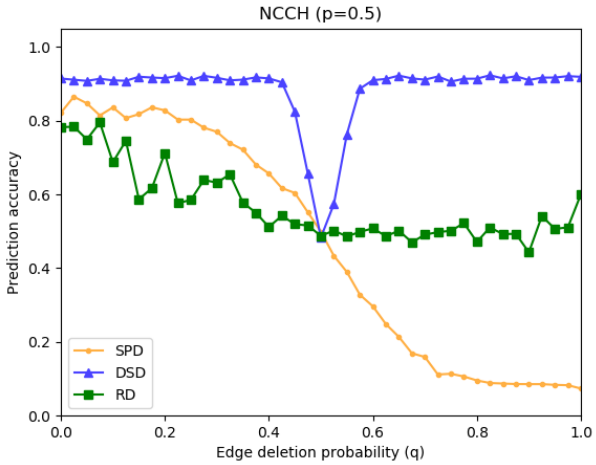

Figure 6.4: Plot showing prediction accuracies of the prediction method using the DSD, SPD, and RD metrics. In this simulation, the parameter p was fixed to 0.5.

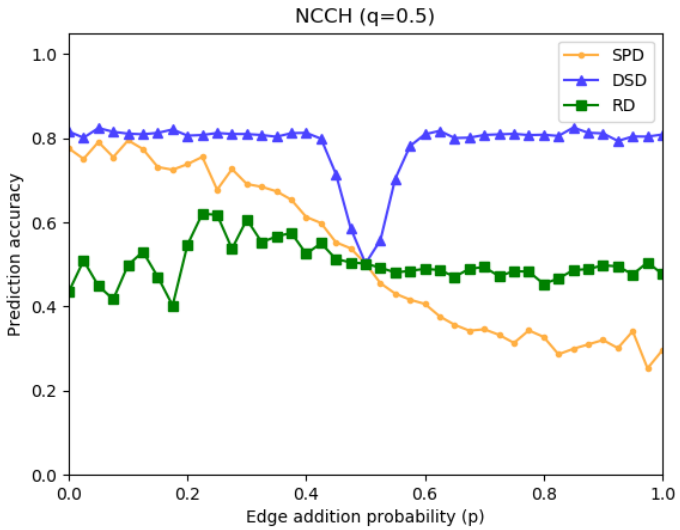

Figure 6.5: Plot showing compressed prediction accuracies for a larger value of the *hubs* parameter. In this simulation, the parameter q was fixed to 0.5, and *hubs* was set to 300.

In order to test the effects of the number of hub nodes added, prediction accuracies were plotted over the *hubs* parameter. Both parameters p and q were set to fixed values such that the prediction accuracies using DSD, SPD, and RD could be clearly separated. Thus a value of $p = 0.2$ and $q = 0.5$ was chosen. These parameters are shown in Table 6.3.

$n\ (= 2m + hubs)$	250
p	0.2
q	0.5
$hubs$	Range from 0 to 400
$hubsP$	0.8
$censorP$	0.7
$avgRuns$	10

Table 6.3: Tables of parameter values used for our NCCH simulations over the *hubs* parameter.

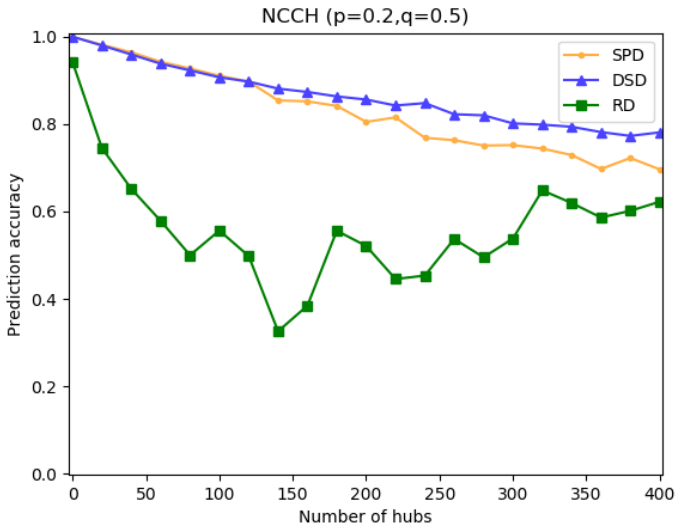

Figure 6.6: Plot showing prediction accuracies over the *hubs* parameter. In this simulation, the parameter p was fixed to 0.2, and q was fixed to 0.5.

6.2.2 Analysis

We can perform a similar analysis to that of the NCC graphs. We can see in Figures 6.3 and 6.4 that the shapes of the prediction accuracy curves do not change significantly. The main difference between these plots and the plots for the NCC graphs are that the plots for NCCH graphs are slightly compressed vertically. This behavior can be explained by the presence of the hub vertices. Since these hub vertices are labeled at random, there will always be a proportion of the vertices in the NCCH graphs that can only be predicted at random. Specifically in the case of Figure 6.3, we see that the prediction accuracies start at 0.9 rather than 1.0. If we consider the number of hub vertices added, $hubs = 100$, in relation the the number of vertices in the NCCH graph, $n = 2m + hubs = 600$, then we can see that since hub vertices will be predicted at random, we should expect a prediction accuracy of around $\frac{550}{600} \approx 0.92$. A simulation run with the parameter $hubs = 300$ was run, and shows this idea of compression in Figure 6.5. The change in the rate of compression can be seen in Figure 6.6.

6.3 Class-weighted Barabási-Albert (CWBA) Graphs

In this section, we construct CWBA graphs (Chapter 3) and run label prediction methods on them. We study the CWBA graphs because they are scale-free.

6.3.1 Data Collection

n	1000
m	Range from 1 to 300
ρ	2
$censorP$	0.7
$avgRuns$	10

(a) Fixed ρ

n	1000
m	300
$\frac{1}{\rho}$	Range from 0.05 to 1
$censorP$	0.7
$avgRuns$	10

(b) Fixed ρ

Table 6.4: Tables of parameter values used in our CWBA simulations. The table on the left shows simulation parameters for a fixed ρ, and the table on the right shows simulation parameters for a fixed m over the inverse of ρ.

Our CWBA graphs have two input parameters, where m is the minimum vertex degree, and ρ is the factor of same-class attachment. Table 6.4 shows the parameters used in our simulation. We also studied the prediction accuracies over $\frac{1}{\rho}$ in order to study the entire range of values for ρ.

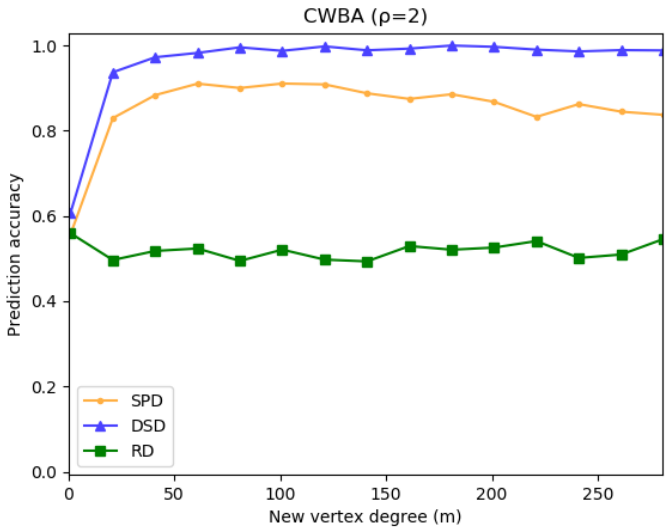

Figure 6.7: Plot showing prediction accuracies over the m parameter. In this simulation, the parameter ρ was fixed to 2.

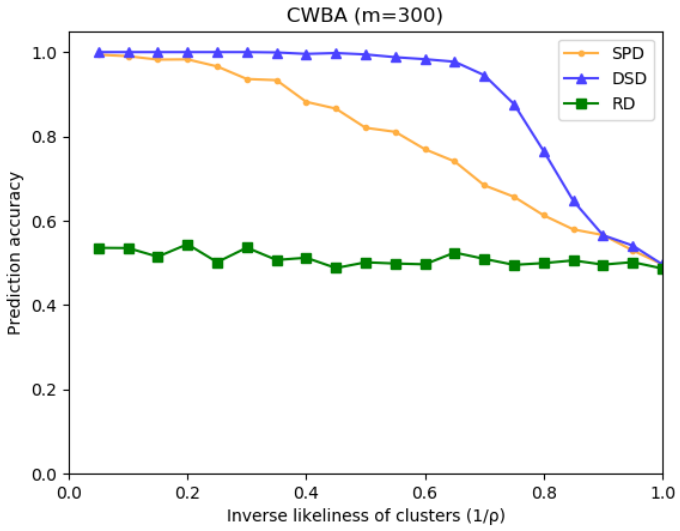

Figure 6.8: Plot showing prediction accuracies over the inverse of the ρ parameter. In this simulation, the parameter m was fixed to 300.

6.3.2 Analysis

In our simulations for the CWBA graph, our initial graph is a star S_m. It is important to discuss the extreme cases for CWBA graphs.

Proposition 6.3. When $\rho = 1$ for CWBA graphs, we get a randomly labeled scale-free graph.

Proof. We note that when $\rho = 1$, the probability of drawing an edge to a vertex u in the CWBA process (Chapter 3) becomes

$$p_u = \begin{cases} \frac{\deg(u)}{w} & : u \in S_l \\ \frac{\deg(u)}{w} & : u \in (V_G - S_l) \end{cases}$$

where

$$w = \sum_{v \in S_l} \deg(v) + \sum_{v \in (V_G - S_l)} \deg(v)$$

We can clearly see that with $\rho = 1$, there is no preference in attachment based on the label, so all vertices are preferentially connected based on the degree of vertices. □

For $\rho = 0$, we can see that vertices with opposite label would only be considered for attachment, and the opposite would be true for extremely high values of ρ.

Figures 6.7 and 6.8 show DSD aids in predicting more accurately than the other two metrics. Figure 6.8 fixes a value for the parameter $m = 300$ and shows prediction accuracies over the entire range of values for the ρ parameter. The figure illustrates that when the same-class preferential attachment factor ρ is 1, the resulting CWBA graph is random, since there is no notion of preferential attachment for $\rho = 1$. However, for $\rho > 1$, drawing same-class edges is preferred which results in a sharp increase in accuracy for the prediction method using DSD, while the method using SPD increases at a linear rate. We must note that the parameter for minimum vertex degree, m, was fixed at $m = 300$, so the resulting CWBA graph is fairly dense. Figure 6.7 shows that increasing the parameter m will not change prediction accuracies for $\rho > 1$, as all of the curves in the plot level out very quickly.

6.4 Overall Findings

After analyzing the results of our simulations, we have found that the shortest path distance (SPD) works well with few paths between clusters. The

diffusion state distance (DSD) works well in general as long as neighborhoods can be distinguished. This can be seen from the NCC and NCCH graph simulations. The resistance distance (RD), however, does not seem to work very well with our simulations, and seems to work best on very sparse graphs.

Chapter 7

Analysis of Real-World Data

In order to test the conclusions of our experimental results, we also performed analyses on two real-world data sets. The Coauthor network contains data about statistician coauthorship in prominent journals, while the email-Eu-Core data set shows email communications within a large research institution. The data sets were picked based upon their relatively small sizes and easy interpretability. In both cases, vertices represent humans, which was done in order to test DSD's performance outside of the biological domain.

Elsewhere, we have used the imprecise term **hub** to refer to the vertices of unusually high degree in certain graphs (see page 11). For the purposes of this chapter only, we will use the following rigorous definition so that we can numerically analyze our data sets.

Definition 7.1. Let G be a graph. A **hub** in G is any vertex v whose degree is more than two standard deviations above the graph average,

$$\deg(v) \geq \mu + 2 * \sum_{u \in G} (\deg(u) - \mu^2)^2$$

where

$$\mu = \frac{1}{|G|} \sum_{u \in G} \deg(u)$$

Under this definition, the number of hubs should be positively correlated with the width of the degree distribution.

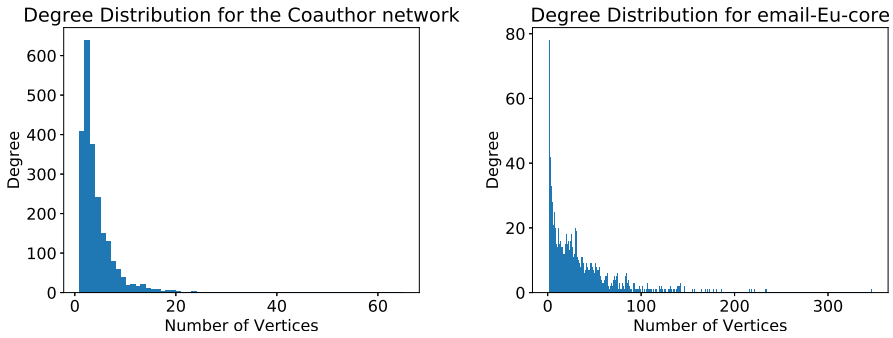

Figure 7.1: The degree distribution plots for both networks. Both plots appear to show scale-free distributions.

7.1 Selected datasets

7.1.1 Coauthor

The Coauthor data set consist of data collected from four leading statistical journals: The Annals of Statistics, Biometrika, the Journal of the American Statistical Association, and the Journal of the Royal Statistical Society. Ji and Jin collected data about all papers published from 2003 through the first half of 2013 and resolved data hygiene issues such as having multiple different published names for the same author. A graph was then constructed where every vertex corresponded to a statistician, and edges were inserted to connect any pair of statisticians who had appeared as coauthors. This graph was then used to cluster the authors into three statistical subdisciplines using a spectral clustering algorithm, SCORE, which stands for Spectral Clustering On Ratios of Eigenvalues [11]. The labels generated by SCORE showed a high degree of agreement with other clustering approaches and were found to be reasonable by human researchers, so we believe they are suitable for use as ground truth labels in a classification experiment. The three labels identified were "Objective Bayes," "Biostatistics," and "High-Dimensional Data Analsysis."

After restricting to the largest connected component, the network has 4388 edges on 2263 vertices, and so is a relatively sparse graph. The average degree is 3.88, while the max is 65. The number of hubs is 98, which is 4.43% of all vertices. This graph appears to have a scale-free degree distribution, as can be seen from Figure 7.1, and so would be expected to have a relatively large number of high-degree hubs.

7.1.2 email-Eu-core

The email-Eu-core data set is built from email data collected over the course of 18 months from 2003 to 2005 at a European research institution. Each vertex corresponds to an employee at the institution, and is labeled an integer indicating that person's department. There are a total of 48 departments in the data set. An edge was drawn between any two parties which exchanged an email over the time period in question [13]. The original version of this data set was directed, but we discard edge direction information for our analysis.

This graph has 986 vertices and 25571 edges after reducing to the largest connected component. The average degree of the graph is 33.9, with the maximum being 347. The number of hubs is 49, which is 4.97% of the entire graph– strikingly similar to the Coauthor network. Also, compared to the Coauthor network, this graph is somewhat smaller and substantially denser, which makes it an attractive candidate for demonstrating the efficacy of DSD, as such a graph would be expected to have more and higher degree hubs than a less dense one.

In addition and in spite of its small size, this graph has 48 possible labels, indicating an average class size of just 20.54 elements. This means that we also have to be more conservative in censoring data on this graph, as it would be easy to censor too high a proportion of one of the smaller classes to be able to accurately recover the labels.

7.2 Results and Analysis

In order to evaluate the efficacy of each classifier, the label prediction experiment was done using 5-fold cross-validation on each predictor. Cross-validation is a common machine learning technique where the point set (in our case, the vertex set of the graph) is divided into k equal-size **folds**. Each fold is censored one at a time, and a trial is run using a predictor built from the uncensored data. These trial accuracies are then averaged in order to compute an overall measurement of accuracy. The primary advantage of cross validation is that it forces prediction to be run on every single vertex of the graph. A disadvantage is that it requires use of small censorship proportions. In this case, 20% of vertices would be censored in each run.

$k = 20$ was used as the parameter for the nearest neighbors algorithm. The results are summarized in the bar plot in Figure 7.2.

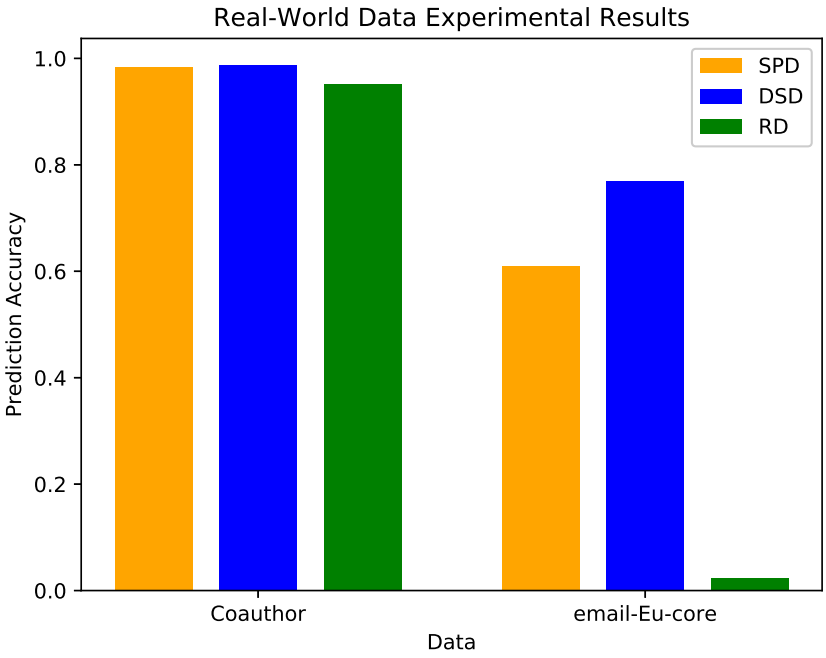

Figure 7.2: Real-world data prediction accuracy results.

The Coauthor results are especially striking, as all three metrics, including resistance distance, performed extremely well. This could probably be explained, at least partially, by the fact that the Coauthor network is fairly sparse and that the number of labels is small. The lower censorship proportion, 20% as compared to the 70% used in the simulated experiments, probably contributes to the high accuracies as well, but informal experiments using random censoring at high proportions yield very similar results.

It seems likely that the high label prediction performance is mostly due to the fact that SCORE was used to generate ground truth. For some reason, the SCORE communities are clustered extremely tightly irrespective of the metric. This is an interesting finding in its own right because it suggests that the way that we think about clusters, at least in the context spectral clustering, probably doesn't capture some important properties of the communities found in real-world data. The fact that resistance distance works well on the spectral clusters but not the real ground truth is especially noteworthy in this regard.

By contrast, the email-Eu-core results are much less surprising. DSD

clearly provides the dominant classification algorithm, followed by a surprisingly strong showing from SPD. RD performs like random guesses, as it did with most of the simulated data (recall that as there are 48 classes, uniform random guessing would yield an expected success rate of 1/48, or about 2.1%).

These results suggest that DSD has some sort of built-in model of community structure which agrees with the real-world data. We expect that these results would generalize to work well with a wide variety of network structures, but particularly those whose topology represents some sort of information exchange.

Chapter 8

Conclusions

Our project hopes to provide information about what makes prediction methods using the diffusion state distance (DSD) metric work better than methods using other metrics on graphs. Our simulation models were constructed to attempt to identify structures within graphs that caused the DSD to work better. In Chapter 3, we proposed the novel Noisy Complete Components (NCC) and Noisy Complete Components with Hubs (NCCH) models in order to see whether tightly clustered graphs and dense neighborhoods would affect prediction using the DSD. We also developed the Class-Weighted Barabási-Albert (CWBA) model in order to see the effects of scale-free properties on prediction using the DSD.

Using our simulation models, we experimented with various parameters of our models in order to get data about changes in prediction accuracy with respect to changes in the graph structure (Chapter 6). We tested parameters that affected neighborhoods of vertices in our models as well as the number of hub vertices. More models could be constructed in future work to draw out characteristics of graph structure that the DSD metric is most affected by. Also, subject-knowledge for specific types of networks, mentioned in Chapter 5, could be added to the models to add to our metric-based clustering algorithm.

Our simulation results show that the DSD is more effective at detecting some properties of graph structure than the shortest path distance and the resistance distance for dense graphs. Prediction methods using the DSD were shown to be more robust to hub vertices and our NCC simulations were able to intuitively show how the DSD determines communities based on neighborhoods rather than direct neighbors. Our project could have included simulations to study the resistance distance metric as well, and graph

models that would cause the DSD metric to cause prediction accuracies to be significantly worse than the shortest path distance.

Our analysis of real-world networks (coauthor, email-Eu-core) did not provide as much information as we expected on how the DSD metric is useful on examples of real networks. However, both still showed that the DSD metric performed best of the three metrics that we studied.

There are many interesting questions remaining. For what parameters for CWBA graphs would the SPD perform better than the DSD? We believe that such an investigation would provide further insight into properties of scale-free networks which would indicate the most appropriate metric for classification problems on scale-free networks. This analysis could also examine other statistics on graphs such as betweenness centrality [15] and eigencentrality based on dissimilarity measures [1] to see whether they are correlated with DSD performance. The effectiveness of the DSD in detecting manifold-like structures of graphs is also a challenge that could be explored. Several simulation models could be constructed to study this question. Also, the effect of the DSD metric in detecting the dispersion of rumors or the spread of information could also be studied. This would relate to the virality of news, products, clothing, and other trends. The way the DSD metric is defined by random walks seems to give a hint for what kinds of real-world data that it should be experimented with. The DSD metric could be compared to heat dispersion and different kinds of dispersions in nature, such as the dispersion of particles or biological dispersion of pollen and seeds. Such studies could provide a more accurate understanding of how natural biological networks interact with each other.

Bibliography

[1] AJ Alvarez-Socorro, GC Herrera-Almarza, and LA González-Díaz. Eigencentrality based on dissimilarity measures reveals central nodes in complex networks. *Scientific reports*, 5:17095, 2015.

[2] Albert-László Barabási and Réka Albert. Emergence of scaling in random networks. *Science*, 286(5439):509–512, 1999.

[3] Mikhail Belkin and Partha Niyogi. Laplacian eigenmaps and spectral techniques for embedding and clustering. In *Advances in neural information processing systems*, pages 585–591, 2002.

[4] Béla Bollobás. *Modern Graph Theory*. Graduate texts in mathematics. Springer, Heidelberg, corrected edition, 1998.

[5] Mengfei Cao, Hao Zhang, Jisoo Park, Noah M. Daniels, Mark E. Crovella, Lenore J. Cowen, and Benjamin Hescott. Going the distance for protein function prediction: A new distance metric for protein interaction networks. *PLOS ONE*, 8(10):1–12, 10 2013.

[6] George Casella and Roger Berger. *Statistical Inference*. Duxbury Resource Center, June 2001.

[7] Michele Catanzaro, Marián Boguñá, and Romualdo Pastor-Satorras. Generation of uncorrelated random scale-free networks. *Phys. Rev. E*, 71:027103, Feb 2005.

[8] Reuven Cohen and Shlomo Havlin. Scale-free networks are ultrasmall. *Phys. Rev. Lett.*, 90:058701, Feb 2003.

[9] Marco Frasca, Alberto Bertoni, Matteo Re, and Giorgio Valentini. A neural network algorithm for semi-supervised node label learning from unbalanced data. *Neural Networks*, 43:84 – 98, 2013.

[10] Zan Huang, Wingyan Chung, and Hsinchun Chen. A graph model for e-commerce recommender systems. *Journal of the American Society for information science and technology*, 55(3):259–274, 2004.

[11] Pengsheng Ji and Jiashun Jin. Coauthorship and citation networks for statisticians. *Ann. Appl. Stat.*, 10(4):1779–1812, 12 2016.

[12] Douglas Klein and Milan Randic. Resistance distance. *Journal of Mathematical Chemistry*, 12:81–95, 12 1993.

[13] Jure Leskovec and Andrej Krevl. SNAP Datasets: Stanford large network dataset collection. `http://snap.stanford.edu/data`, June 2014.

[14] C. D. (Carl Dean) Meyer. *Matrix analysis and applied linear algebra.* Society for Industrial and Applied Mathematics, Philadelphia, c2000.

[15] Mark EJ Newman. A measure of betweenness centrality based on random walks. *Social networks*, 27(1):39–54, 2005.

[16] Duncan J. Watts and Steven H. Strogatz. Collective dynamics of 'small-world' networks. *Nature*, 393(6684):440–442, June 1998.

[17] Eric W. Weisstein. Resistance distance. From MathWorld—A Wolfram Web Resource. Last visited on 04/24/2019.